Universal analytic expression of electric-dipole matrix elements for carbon nanotubes

Abbas Zarifi[1,*] and Thomas Garm Pedersen[2]
[1]*Department of Physics, Yasouj University, Yasouj, Iran*
[2]*Department of Physics and Nanotechnology, Aalborg University, Aalborg, Denmark*
(Received 5 July 2009; revised manuscript received 11 October 2009; published 30 November 2009)

The optical properties of carbon nanotubes strongly depend on the polarization direction of the incident light. The challenge of describing the optical properties analytically is mainly associated with the calculation of dipole matrix elements. Although an analytic expression has been obtained for dipole matrix elements for light polarized parallel to the nanotube axis no expression has been found so far for the perpendicular case. Based on the structural symmetry we obtain an analytic expression for the electric-dipole matrix elements of single wall carbon nanotubes with arbitrary chirality for linearly polarized light with polarization perpendicular to the nanotube axis. This expression is used to calculate the short axis linear susceptibility semianalytically. Excellent agreement with numerical calculations is demonstrated.

DOI: 10.1103/PhysRevB.80.195422 PACS number(s): 78.67.Ch, 78.67.Bf, 73.22.−f

I. INTRODUCTION

The optical properties of carbon nanotubes (CNs) have been studied extensively both experimentally[1–4] and theoretically.[5–15] Notably, the polarization-dependent optical properties of these nanomaterials have been investigated in many aspects and in different ranges of energy.[2,6,13,16–18] Because of their nanometer-sized diameter and a micron-sized length, CNs are quasi-one-dimensional systems. Due to their one dimensionality, their optical response strongly depends on the polarization direction of the incident light with respect to the nanotube axis. Moreover, the polarization absorption coefficient of CN fiber for electric field parallel and perpendicular to the fiber axis have become experimentally accessible.[19–22] Therefore, a study of the polarization dependence of the optical matrix elements is required. A few theoretical papers have investigated the optical properties of CNs for light polarized parallel to the nanotube axis analytically.[12–15] However, for polarization perpendicular to the axis no analytic calculation for CNs with arbitrary chirality has been done so far. In our previous work,[12] we have investigated the linear susceptibility of zigzag CNs for light polarized both parallel and perpendicular to the nanotube axis. We have managed to find closed form analytic expressions for electric dipole matrix elements for polarization both parallel and perpendicular to the nanotube axis. The optical matrix elements of semiconducting CNs around the K (K') points of the two-dimensional (2D) Brillouin zone have been investigated analytically by Goupalov,[13] who has studied the dependence of the optical matrix elements on the nanotube chirality and excitation energy as well as the allowed transitions in each case of polarizations. However, a full form for the calculation of the electric-dipole matrix elements has not been obtained. Our calculations clearly show the selection rules governing the transitions and moreover provide an analytic expression for the electric dipole matrix applicable to all band to band transitions. Jiang and co-workers[14] have investigated the dipole matrix elements for light polarized both parallel and perpendicular to the nanotube axis. They have obtained an analytic expression for the parallel case for CNs with arbitrary chirality and, moreover, derived an expression for the perpendicular case valid for armchair CNs but only near the Fermi level. However, their method does not exploit fully the structural symmetry of CNs as evidenced by the fact that different matrix elements are obtained for allowed degenerate transitions. Hence, it is difficult to apply to chiral CNs. In this paper, we obtain analytic expression for electric-dipole matrix elements for light polarized perpendicular to the nanotube axis for CNs with arbitrary chirality. This universal expression is reduced to even simpler forms for the cases of zigzag and armchair CNs. We use the obtained expression to investigate the short axis linear susceptibility for CNs with arbitrary chirality semianalytically. Moreover, it could be used to study the linear and nonlinear optical properties of SWCNs. The tight-binding method has been used in our calculations to find the dipole matrix elements for light polarized perpendicular to the nanotube axis has included neither the exciton effect nor depolarization effect. Our aim is to find an analytic expression for dipole matrix elements originating from all band to band transitions for CNs with arbitrary chirality. Apparently, this is only possible in the simple noninteracting case.

II. ENERGY DISPERSION RELATION FOR CARBON NANOTUBES

The electronic properties of single walled carbon nanotubes (SWCNs) within the single-particle approximation are often described by the tight-binding approximation.[23–27] Taking into account the nearest neighbor interaction when combined with a zone-folding approximation the tight-binding model yields analytic expression for the electronic band structure of CNs. Figure 1 shows the atom A at the origin and its three nearest neighbor B atoms in the hexagonal lattice of graphene along with the rotated coordinate system (X,Y) in the circumferential and axial directions, respectively.

To make a tube, the translational vector $\vec{T}$ will be in the direction of the nanotube axis and the chiral vector $\vec{C}$ in the circumferential direction. Hence, we consider the Y axis parallel to the translational vector and X axis in the circumferential direction in order that the wave numbers K_1 and K_2 provide the circumferential and axial components of the

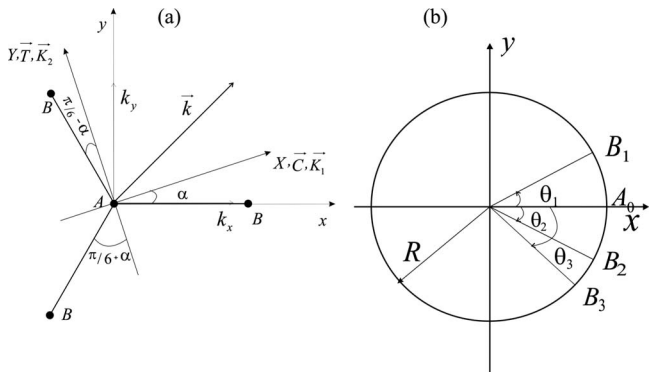

FIG. 1. (a) Unrolled positions of an A atom at the origin and its three nearest neighbor B atoms. The angle between the bonds and the chiral $\vec{C}$ and translational $\vec{T}$ vectors are also shown. The components X and Y of the rotated coordinate system are chosen in the direction of the circumferential and translational vectors, respectively. (b) Rolled-up positions for an A atom at the origin (A_0) and its three nearest-neighbor B atoms.

wave vector, respectively. We ignore the mixing of π and σ orbitals due to the curvature of the nanotube and thus consider only π bands, as curvature effects are of minor importance for all but the smallest CNs. Following Ref. 27, the nonzero Hamiltonian elements $H_{BA}(\vec{k})=H_{AB}^{*}(\vec{k})$ are given by

$$H_{AB}(\vec{k}) = \gamma_0 f(\vec{k}),$$

$$f(\vec{k}) = \sum_{l=1}^{3} e^{-i\vec{k}\cdot\vec{b}_l^A} = e^{-ik_x a/\sqrt{3}} + 2e^{ik_x a/(2\sqrt{3})}\cos(k_y a/2), \quad (1)$$

where $a=2.46$ Å is the lattice constant of graphene, $\gamma_0 \approx 2.89$ eV is the nearest neighbor overlap integral, $\vec{b}_l^A$ $(l=1,2,3)$ are the nearest-neighbor carbon atom vectors from A to B sites,[27] and

$$k_x = K_1\cos(\alpha) - K_2\sin(\alpha),$$

$$k_y = K_1\sin(\alpha) + K_2\cos(\alpha), \quad (2)$$

where $\alpha=\pi/6-\cos^{-1}[(2n+m)/(2\sqrt{n^2+m^2+nm})]$, where m and n designate the chiral indices of the CN in the usual notation.[27] Hence, solving the 2×2 Hamiltonian matrix equation, the energy eigenvalues are obtained as a function of α, K_1, and K_2 given by

$$E_{c,v}(\vec{k}) = \pm\,\gamma_0|f(\vec{k})|, \quad (3)$$

where

$$|f(\vec{k})| = \sqrt{3 + 2\cos(k_y a) + 4\cos(k_y a/2)\cos(\sqrt{3}k_x a/2)}. \quad (4)$$

For all arbitrary (n,m) CNs the allowed wave vector components K_1^{μ} in the circumferential direction are defined by

$$K_1^{\mu}L = 2\pi\mu, \quad \mu = 0,\ldots,N-1, \quad (5a)$$

and

$$-\pi/T \le K_2 \le \pi/T. \quad (5b)$$

Here, L is the length of the nanotube circumference and N the number of hexagons in the nanotube unit cell. The corresponding normalized eigenvectors are

$$v(\vec{k}) = (C_{vA}, C_{vB}) = \frac{1}{\sqrt{2}}(-e^{i\varphi_v}, 1),$$

$$c(\vec{k}) = (C_{cA}, C_{cB}) = \frac{1}{\sqrt{2}}(e^{i\varphi_c}, 1) \quad (6)$$

in which $\varphi_{v,c}$, as the argument of the quantity $e^{-ik_x b}+2e^{ik_x b/2}\cos(\sqrt{3}bk_y/2)$, is defined by

$$\varphi_{v,c} = \tan^{-1}\left(\frac{2\cos(k_y b\sqrt{3}/2)\sin(k_x b/2) - \sin(k_x b)}{2\cos(k_y b\sqrt{3}/2)\cos(k_x b/2) + \cos(k_x b)}\right). \quad (7)$$

III. ELECTRIC DIPOLE VECTOR FOR CARBON NANOTUBES

Denoting the valence bands by v and the conduction bands by c, the electric-dipole vector between an initial valence and a final conduction state is given by

$$\vec{d}_{c\vec{k}',v\vec{k}} = -e\langle\psi_c(\vec{k}',\vec{r})|\vec{r}|\psi_v(\vec{k},\vec{r})\rangle. \quad (8)$$

Here, $e>0$ is the elementary charge. As the functions $\psi_{v,c}(\vec{k},\vec{r})$ are the eigenfunctions of the unperturbed Hamiltonian operator, one can write

$$\langle\psi_c(\vec{k}',\vec{r})|\vec{r}|\psi_v(\vec{k},\vec{r})\rangle = \frac{1}{E_c(\vec{k}') - E_v(\vec{k})}\langle\psi_c(\vec{k}',\vec{r})|[\hat{H},\vec{r}]|\psi_v(\vec{k},\vec{r})\rangle, \quad (9)$$

in which $[\hat{H},\vec{r}]=\hat{H}\vec{r}-\vec{r}\hat{H}$. Expanding the eigenfunctions $\psi_{v,c}(\vec{k},\vec{r})$ by a linear combination of Bloch functions $\Phi_s(\vec{k},\vec{r})=\frac{1}{\sqrt{N}}\Sigma_l^N e^{i\vec{k}\cdot\vec{R}_{ls}}\varphi(\vec{r}-\vec{R}_{ls})$, where N is the number of unit cells, $\varphi(\vec{r}-\vec{R})$ denotes the atomic π-electron wave function, $\vec{R}_{ls}$ is the position vector for each l carbon atoms in the sth unit cell, and introducing the completeness relation $\Sigma_{pq}|\varphi(\vec{r}-\vec{R}_{pq})\rangle\langle\varphi(\vec{r}-\vec{R}_{pq})|=1$ between $\hat{H}$ and $\vec{r}$, Eq. (9) can be written

$$\langle\psi_c(\vec{k}',\vec{r})|\vec{r}|\psi_v(\vec{k},\vec{r})\rangle = \frac{1}{E_{cv}(\vec{k}',\vec{k})}\frac{1}{N}\sum_{ij} C_{ci}^{*}(\vec{k}')C_{vj}(\vec{k}) \times\sum_{st} e^{-i\vec{k}'\cdot\vec{R}_{si}}e^{i\vec{k}\cdot\vec{R}_{tj}} \times(\vec{R}_{tj}-\vec{R}_{si})\langle\varphi(\vec{r})|\hat{H}|\varphi[\vec{r}-(\vec{R}_{tj}-\vec{R}_{si})]\rangle, \quad (10)$$

where $E_{cv}(\vec{k}',\vec{k})=E_c(\vec{k}')-E_v(\vec{k})$ and the expansion coefficients $C_{ci}(\vec{k})$ and $C_{vj}(\vec{k})$ are the eigenstates of conduction and valence bands. Here, we have changed the variable of

integration from $\vec{r}$ to $\vec{r}'=\vec{r}-\vec{R}_{si}$ and after that dropped the prime on the dummy integration variable $\vec{r}'$ for convenience. Equation (10) is a general equation for any arbitrary unit cell with any number of atoms. We will now apply this equation to the substructure containing an A and B atom in the graphene unit cell and then applying boundary conditions to generate the corresponding result for CNs. Hence, considering only the three nearest-neighbor atoms, Eq. (10) is written

$$\langle\psi_c(\vec{k}',\vec{r})|\vec{r}|\psi_v(\vec{k},\vec{r})\rangle = \frac{1}{NE_{cv}(\vec{k}',\vec{k})}\Bigg\{C^*_{cA}(\vec{k}')C_{vB}(\vec{k})\sum_{st} e^{-i\vec{k}'\cdot\vec{R}_{sA}}e^{i\vec{k}\cdot\vec{R}_{tB}}(\vec{R}_{tB}-\vec{R}_{sA})\langle\varphi(\vec{r})|\hat{H}|\varphi[\vec{r}-(\vec{R}_{tB}-\vec{R}_{sA})]\rangle$$
$$+ C^*_{cB}(\vec{k}')C_{vA}(\vec{k})\sum_{st} e^{-i\vec{k}'\cdot\vec{R}_{sB}}e^{i\vec{k}\cdot\vec{R}_{tA}}(\vec{R}_{tA}-\vec{R}_{sB})\langle\varphi(\vec{r})|\hat{H}|\varphi[\vec{r}-(\vec{R}_{tA}-\vec{R}_{sB})]\rangle\Bigg\}. \tag{11}$$

Introducing $\vec{R}_{tB}=\vec{R}_{sA}+\vec{b}^A_l$ and $\vec{R}_{tA}=\vec{R}_{sB}+\vec{b}^B_l$, where $\vec{b}^A_l$ and $\vec{b}^B_l$ $(l=1,2,3)$ are the nearest-neighbor carbon atom vectors from A to B and B to A sites, respectively, and $|\vec{b}^A_l|=|\vec{b}^B_l|=|\vec{b}_l|=a_{C-C}=a/\sqrt{3}$ is the bond length, one has

$$\langle\psi_c(\vec{k}',\vec{r})|\vec{r}|\psi_v(\vec{k},\vec{r})\rangle = \frac{1}{NE_{cv}(\vec{k}',\vec{k})}\Bigg\{C^*_{cA}(\vec{k}')C_{vB}(\vec{k})\sum_{s}\sum_{l=1}^{3} e^{i(\vec{k}-\vec{k}')\cdot\vec{R}_{sA}}e^{i\vec{k}\cdot\vec{b}^A_l}\vec{b}^A_l\langle\varphi(\vec{r})|\hat{H}|\varphi(\vec{r}-\vec{b}^A_l)\rangle$$
$$+ C^*_{cB}(\vec{k}')C_{vA}(\vec{k})\sum_{s}\sum_{l=1}^{3} e^{i(\vec{k}-\vec{k}')\cdot\vec{R}_{sB}}e^{i\vec{k}\cdot\vec{b}^B_l}\vec{b}^B_l\langle\varphi(\vec{r})|\hat{H}|\varphi(\vec{r}-\vec{b}^B_l)\rangle\Bigg\}. \tag{12}$$

Introducing atomic dipole vectors $\vec{v}^{A,B}$ as:

$$\vec{v}^A(\vec{k}) = -\sum_{l=1}^{3} e^{-i\vec{k}\cdot\vec{b}^A_l}\vec{b}^A_l, \quad \vec{v}^B(\vec{k}) = -\sum_{l=1}^{3} e^{-i\vec{k}\cdot\vec{b}^B_l}\vec{b}^B_l, \tag{13}$$

and replacing $\vec{b}^A_l$ and $\vec{b}^B_l$ by $-\vec{b}^A_l$ and $-\vec{b}^B_l$ in Eq. (12), respectively, we obtain the general form of the electric dipole vector:

$$\vec{d}_{c\vec{k}',v\vec{k}} = \frac{-e\gamma_0}{NE_{cv}(\vec{k}',\vec{k})}\Bigg\{C^*_{cA}(\vec{k}')C_{vB}(\vec{k})\sum_{s} e^{i(\vec{k}-\vec{k}')\cdot\vec{R}_{sA}}\vec{v}^A(\vec{k})$$
$$+ C^*_{cB}(\vec{k}')C_{vA}(\vec{k})\sum_{s} e^{i(\vec{k}-\vec{k}')\cdot\vec{R}_{sB}}\vec{v}^B(\vec{k})\Bigg\}, \tag{14}$$

where again $\gamma_0=\langle\varphi(\vec{r})|\hat{H}|\varphi(\vec{r}+\vec{b}^{A,B}_l)\rangle$ for three nearest-neighbor atoms. Equation (14) is in full agreement with Eq. (8) in Ref. 14 where they have obtained the momentum matrix element instead of the electric dipole matrix element. It is mentioned that the second term of Eq. (14) is not the complex conjugate of the first term. Equation (14) can be used to find the dipole matrix elements for both parallel and perpendicular polarizations in CNs. In the case of parallel polarization, all A atoms in different cells have the same component of the atomic dipole vector and similarly for all B atoms. Hence, Eq. (14) is readily simplified for parallel polarization.[14,28] For the case of perpendicular polarization one needs to consider the phase difference between atoms A in different cells and B atoms as well. In this case, we have obtained a closed form analytic expression for zigzag CNs.[12] Using an expression similar to Eq. (14), Jiang and coworkers have presented a method to obtain the dipole vector for armchair CNs[14] for the case of perpendicular polarization and have obtained an expression to linear order in Δk_x and Δk_y. However, because the full structural symmetry of the system has not been taken into account, their method is difficult to apply for arbitrary chiral CNs. Below, we derive an analytic expression for the perpendicular case of the electric-dipole vector for SWCNs with arbitrary chirality and its behavior for the important subclasses of zigzag and armchair CNs is discussed. Subsequently we use this expression to find the short-axis linear susceptibility for SWCNs.

IV. PERPENDICULAR POLARIZATION

Using Eq. (14), the x component of the electric dipole vector is given by

$$d^x_{c\vec{k}',v\vec{k}} = \frac{-e\gamma_0}{NE_{cv}(\vec{k}',\vec{k})}\Bigg\{C^*_{cA}(\vec{k}')C_{vB}(\vec{k})\sum_{s} e^{i(\vec{k}-\vec{k}')\cdot\vec{R}_{sA}}v^A_x(\vec{k})$$
$$+ C^*_{cB}(\vec{k}')C_{vA}(\vec{k})\sum_{s} e^{i(\vec{k}-\vec{k}')\cdot\vec{R}_{sB}}v^B_x(\vec{k})\Bigg\}. \tag{15}$$

In fact the cylindrical symmetry makes it more convenient to work with right and left handed operators v_+ and v_-, respectively, defined by $v_\pm=v_x\pm iv_y$. For CNs with arbitrary integers (n,m), the x and y components of $\vec{v}^A$ and $\vec{v}^B$ for any arbitrary A and B atoms based on a chosen A_0 atom and its three nearest neighbors as B_0 atoms shown in Fig. 1(b) are given by

$$v_x^A(\phi_j) = \frac{1}{2}[e^{i\phi_j}v_+^{A_0}(\vec{k}) + e^{-i\phi_j}v_-^{A_0}(\vec{k})],$$

$$v_y^A(\phi_j) = \frac{-i}{2}[e^{i\phi_j}v_+^{A_0}(\vec{k}) - e^{-i\phi_j}v_-^{A_0}(\vec{k})],$$

$$v_x^B(\phi_j) = \frac{-1}{2}[e^{i\phi_j}v_+^{B_0}(\vec{k}) + e^{-i\phi_j}v_-^{B_0}(\vec{k})],$$

$$v_y^B(\phi_j) = \frac{i}{2}[e^{i\phi_j}v_+^{B_0}(\vec{k}) - e^{-i\phi_j}v_-^{B_0}(\vec{k})]. \quad (16)$$

Here, $\phi_j = 2\pi j/N$, $(j=0,1,\ldots,N-1)$ is the phase difference between two A sites or two B sites respectively. Inserting Eq. (16) into Eq. (15), one obtains

$$d^x_{c\vec{k}',v\vec{k}} = \frac{-e\gamma_0}{2NE_{cv}(\vec{k}',\vec{k})}\Bigg\{C^*_{cA}(\vec{k}')C_{vB}(\vec{k})\sum_s e^{i(\vec{k}-\vec{k}')\cdot\vec{R}_{sA}}e^{i\phi_j}v_+^{A_0}(\vec{k})$$
$$- C^*_{cB}(\vec{k}')C_{vA}(\vec{k})\sum_s e^{i(\vec{k}-\vec{k}')\cdot\vec{R}_{sB}}e^{i\phi_j}v_+^{B_0}(\vec{k})$$
$$+ C^*_{cA}(\vec{k}')C_{vB}(\vec{k})\sum_s e^{i(\vec{k}-\vec{k}')\cdot\vec{R}_{sA}}e^{-i\phi_j}v_-^{A_0}(\vec{k})$$
$$- C^*_{cB}(\vec{k}')C_{vA}(\vec{k})\sum_s e^{i(\vec{k}-\vec{k}')\cdot\vec{R}_{sB}}e^{-i\phi_j}v_-^{B_0}(\vec{k})\Bigg\}. \quad (17)$$

Using the fact that $e^{i(\vec{k}-\vec{k}')\cdot\vec{R}_{sA}} = e^{i(\vec{K}_2-\vec{K}'_2)\cdot\vec{R}_{sA}}e^{i(2\pi\mu-2\pi\mu')j/N}$ and simplifying Eq. (17), one obtains

$$d^x_{c\vec{k}',v\vec{k}} = \frac{-e\gamma_0\delta_{\vec{K}_2\vec{K}'_2}}{2E_{cv}(\vec{k}',\vec{k})}[\{C^*_{cA}(\vec{k}')C_{vB}(\vec{k})v_+^{A_0}(\vec{k})$$
$$- C^*_{cB}(\vec{k}')C_{vA}(\vec{k})v_+^{B_0}(\vec{k})\}\delta_{\mu'=\mu+1}$$
$$+ \{C^*_{cA}(\vec{k}')C_{vB}(\vec{k})v_-^{A_0}(\vec{k})$$
$$- C^*_{cB}(\vec{k}')C_{vA}(\vec{k})v_-^{B_0}(\vec{k})\}\delta_{\mu'=\mu-1}]. \quad (18a)$$

The y component of the electric dipole vector is obtained by exploiting Eq. (14) once more and do the calculation in a similar manner to that of the x component, hence,

$$d^y_{c\vec{k}',v\vec{k}} = \frac{ie\gamma_0\delta_{\vec{K}_2\vec{K}'_2}}{2E_{cv}(\vec{k}',\vec{k})}[\{C^*_{cA}(\vec{k}')C_{vB}(\vec{k})v_+^{A_0}(\vec{k})$$
$$- C^*_{cB}(\vec{k}')C_{vA}(\vec{k})v_+^{B_0}(\vec{k})\}\delta_{\mu'=\mu+1}$$
$$- \{C^*_{cA}(\vec{k}')C_{vB}(\vec{k})v_-^{A_0}(\vec{k})$$
$$- C^*_{cB}(\vec{k}')C_{vA}(\vec{k})v_-^{B_0}(\vec{k})\}\delta_{\mu'=\mu-1}]. \quad (18b)$$

Comparing Eqs. (18a) and (18b), the following relations between $d^x_{c\vec{k},v\vec{k}'}$ and $d^y_{c\vec{k},v\vec{k}'}$ are established. For $\mu'=\mu+1$ case, $d^y_{c\vec{k},v\vec{k}'} = -id^x_{c\vec{k},v\vec{k}'}$ and for $\mu'=\mu-1$ case, $d^y_{c\vec{k},v\vec{k}'} = id^x_{c\vec{k},v\vec{k}'}$. Furthermore, these equations show that the transitions $E^v_\mu(k) \to E^c_{\mu\pm1}(k)$ are the allowed for the case of perpendicular polarization. These relations previously have been shown for armchair CNs in Ref. 14.

The next and most important step is to find $v_\pm^{A_0}$ and $v_\pm^{B_0}$ for SWCNs with arbitrary chirality. To this end, we have selected a 3D coordinate system, Fig. 1(b), where the z axis normal to the plane indicates the nanotube axis and the x axis is defined in such a way that it passes through an A atom, called A_0. We note that because of the full symmetry of the system there is no priority for choosing A_0 as a reference site over the B_0 site. When a graphene layer is rolled up around the Y axis (translational vector) in Fig. 1(a), the positions of the three nearest-neighbor atoms is the same as shown in Fig. 1(b). By fixing atom A_0 on the x axis so that $x_{A_0}=R$ and $y_{A_0}=0$, where R is the radius of the nanotube, one can easily find the components of the vectors $\vec{b}_l^{A_0}$ and $\vec{b}_l^{B_0}$, given by

$$b_{ix}^{A_0} = R\cos(\theta_i) - R, \quad i=1,2,3,$$

$$b_{1y}^{A_0} = R\sin(\theta_1), \quad b_{2y}^{A_0} = -R\sin(\theta_2), \quad b_{3y}^{A_0} = -R\sin(\theta_3),$$

$$b_{ix}^{B_0} = -b_{ix}^{A_0}, \quad b_{iy}^{B_0} = -b_{iy}^{A_0}. \quad (19)$$

Here, the associated angles of the three nearest neighbor atoms are given by

$$\theta_1 = \frac{S_{A_0B_1}}{R} = \frac{\pi(n+m)}{n^2+m^2+nm},$$

$$\theta_2 = \frac{S_{A_0B_2}}{R} = \frac{\pi m}{n^2+m^2+nm},$$

$$\theta_3 = \frac{S_{A_0B_3}}{R} = \frac{\pi n}{n^2+m^2+nm}. \quad (20)$$

Inserting Eqs. (19) into the Eq. (13) the x and y components of the atomic dipole vectors $\vec{v}^{A_0,B_0}(\vec{k})$ are given by

$$v_x^{A_0}(\vec{k}) = -\sum_{l=1}^{3} e^{-i\vec{k}\cdot\vec{b}_l^{A_0}}b_{lx}^{A_0}$$
$$= -R\{e^{-ik_xb}[\cos(\theta_1)-1] + e^{ik_xb/2-ik_yb\sqrt{3}/2}[\cos(\theta_2)-1]$$
$$+ e^{ik_xb/2+ik_yb\sqrt{3}/2}[\cos(\theta_3)-1]\},$$

$$v_y^{A_0}(\vec{k}) = -\sum_{l=1}^{3} e^{-i\vec{k}\cdot\vec{b}_l^{A_0}}b_{ly}^{A_0}$$
$$= R\{-e^{-ik_xb}\sin(\theta_1) + e^{ik_xb/2-ik_yb\sqrt{3}/2}\sin(\theta_2)$$
$$+ e^{ik_xb/2+ik_yb\sqrt{3}/2}\sin(\theta_3)\},$$

$$v_x^{B_0}(\vec{k}) = -v_x^{A_0*}(\vec{k}), \quad v_y^{B_0}(\vec{k}) = -v_y^{A_0*}(\vec{k}). \quad (21)$$

Using the relation $v_\pm^{A_0} = (v_x^{A_0} \pm iv_y^{A_0})$ one has

$$v_\pm^{A_0} = R\{e^{-ik_xb}(1-e^{\pm i\theta_1}) + e^{ik_xb/2-ik_yb\sqrt{3}/2}(1-e^{\mp i\theta_2})$$
$$+ e^{ik_xb/2+ik_yb\sqrt{3}/2}(1-e^{\mp i\theta_3})\}. \quad (22a)$$

As mentioned, exploiting the full symmetric of the system one can easily obtain the expressions for $v_\pm^{B_0}$

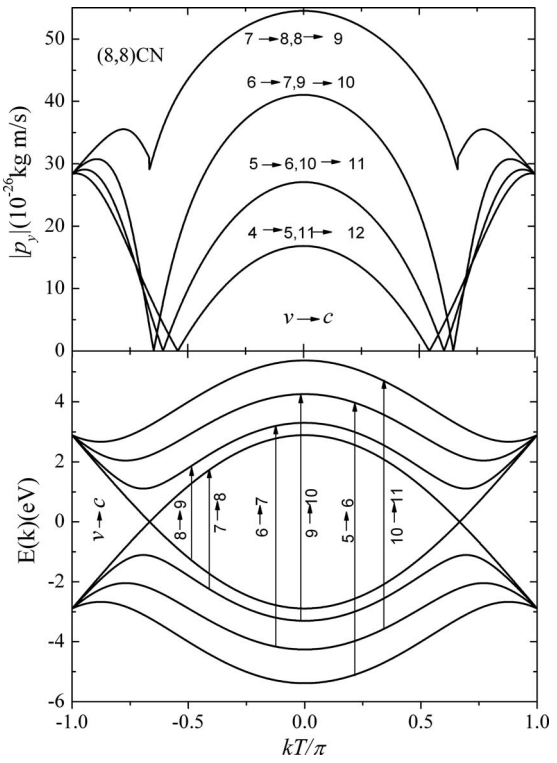

FIG. 2. k dependence of $|p_y|$ for a (8, 8) CN for some allowed transitions. Transitions are labeled with respect to the quantum numbers introduced in Eq. (5a).

$$
\begin{aligned}
v_{\pm}^{B_0} &= -v_{\pm}^{A_0*} \\
&= -R\{e^{ik_x b}(1-e^{\mp i\theta_1}) + e^{-ik_x b/2+ik_y b\sqrt{3}/2}(1-e^{\pm i\theta_2}) \\
&\quad + e^{-ik_x b/2-ik_y b\sqrt{3}/2}(1-e^{\pm i\theta_3})\}. \qquad (22b)
\end{aligned}
$$

For simplicity we write $v_{\pm}^{A_0}=-v_{\pm}^{B_0*}=|v_{\pm}^{A_0}|e^{i\varphi_{\pm}}$, in which $\varphi_{\pm}$, as the argument of the $v_{\pm}^{A_0}$, is given by $\varphi_{\pm}=\arctan(X_{\pm}/Y_{\pm})$, where

$$
\begin{aligned}
X_{\pm} &= -\sin(b_1)[1-\cos(\theta_1)] \mp \sin(\theta_1)\cos(b_1) \\
&\quad + \sum_{i=2}^{3}\{\sin(b_i)[1-\cos(\theta_i)] \pm \sin(\theta_i)\cos(b_i)\} \\
Y_{\pm} &= \sum_{i=1}^{3}\{\cos(b_i)[1-\cos(\theta_i)] \mp \sin(\theta_i)\sin(b_i)\}. \qquad (23)
\end{aligned}
$$

Using the eigenvector equations Eq. (6) and atomic dipole vector Eq. (22b) and inserting into Eq. (18a) and (18b) we obtain closed form expressions for the x and subsequently y components of the electric-dipole matrix elements, given by

$$
\begin{aligned}
|d^x_{c\vec{k}',v\vec{k}}| &= |d^y_{c\vec{k}',v\vec{k}}| \\
&= \frac{e\gamma_0|v_{\pm}^{A_0}|\delta_{\vec{K}_2\vec{K}_2'}}{2E_{cv}(\vec{k}',\vec{k})} \\
&\quad \times \left|\sin\left[\frac{2\varphi_{\pm}(\vec{k})-\varphi_c(\vec{k}')-\varphi_v(\vec{k})}{2}\right]\right| \delta_{\mu'=\mu\pm1}. \qquad (24)
\end{aligned}
$$

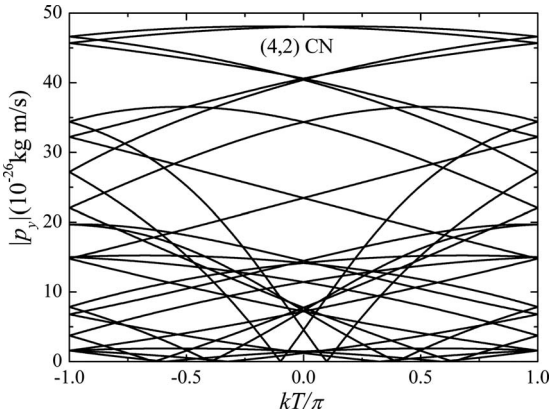

FIG. 3. k dependence of $|p_y|$ for (4, 2) CN for all allowed transitions.

Equation (24) is the main result of this paper. It gives the absolute value of the electric dipole matrix elements for arbitrary (n,m) SWCNs as a function of wave vector and chiral angle. The equation indicates that for perpendicular polarization, electric transitions are allowed between valance and conduction states with the same 1D wave vector $(\delta_{\vec{K}_2\vec{K}_2'})$ but different energy subband indices μ and μ' differing by ±1.

Applying values $\alpha=\pi/6$, $\theta_1=\theta_3=\frac{\pi}{n}$, $\theta_2=0$, $k_x=[K_1\sqrt{3}/2-K_2/2]$, and $k_y=[K_1/2+K_2\sqrt{3}/2]$ for zigzag CNs, one simply obtains $v_{\pm}^{A_0}=2\,\mathrm{Re}^{ibK_2/2}\,\mathrm{Re}[(1-e^{\pm i\pi/n})e^{-ib(K_1\sqrt{3})/2}]$ and $2\varphi_{\pm}(\vec{k})=bK_2=aK_2/\sqrt{3}$. Therefore, for zigzag CNs, we obtain $|v_{\pm}^{A_0}|=2R\times\mathrm{Re}[(1-e^{\pm i\pi/n})e^{-ib(K_1\sqrt{3})/2}]=2R|\cos(\mu\pi/n)-\cos(\mu'\pi/n)|$. Using these expressions, Eq. (24) is found to be in a full agreement with our previous work.[12] The expression for $|v_{\pm}^{A_0}|$ is k independent for zigzag CNs but depends on k for armchair and chiral CNs. We plot the absolute value of the momentum matrix element $p_y=(m_e/\hbar e)E_{cv}(\vec{k}',\vec{k})|d^y_{c\vec{k}',v\vec{k}}|$ for the important transitions near the band gap of a (8, 8) CN in Fig. 2. According to the energy dispersion relation, one can easily see that transitions from valence to conduction bands $(v\rightarrow c)$ denoted by $9\rightarrow10$ and $6\rightarrow7$ are equal and this is also the case for the transitions $8\rightarrow9$, $7\rightarrow8$ and $5\rightarrow6$, $10\rightarrow11$. Therefore, each group of the transitions has exactly the same value of the momentum matrix element as shown in the plot. These bands are separated only in the presence of a constant magnetic field. Our plot in Fig. 2 for armchair CNs basically is similar to that of Fig. 6 in Ref. 14. However looking carefully at Fig. 6 in Ref. 14 it is seen that allowed degenerate transitions have created different matrix elements. For example degenerate transitions such as $10\rightarrow11$, $9\rightarrow10$ have led to different matrix elements, which would not be the case if the full symmetry were exploited. Other degenerate transitions such as $11\rightarrow12$, $8\rightarrow9$, and $12\rightarrow13$, $7\rightarrow8$ also have produced different matrix elements.

We note that the matrix elements obtained in Ref. 14 cannot give a correct result for obtaining optical properties of CNs e.g., linear susceptibility. By using the same method for chiral CNs it clearly breaks the symmetry of the system. In fact, the definition of nearest-neighbor atoms is not consistent with Eq. (7) in that paper. To make clear the symmetry of our calculation we plot the absolute value of the momen-

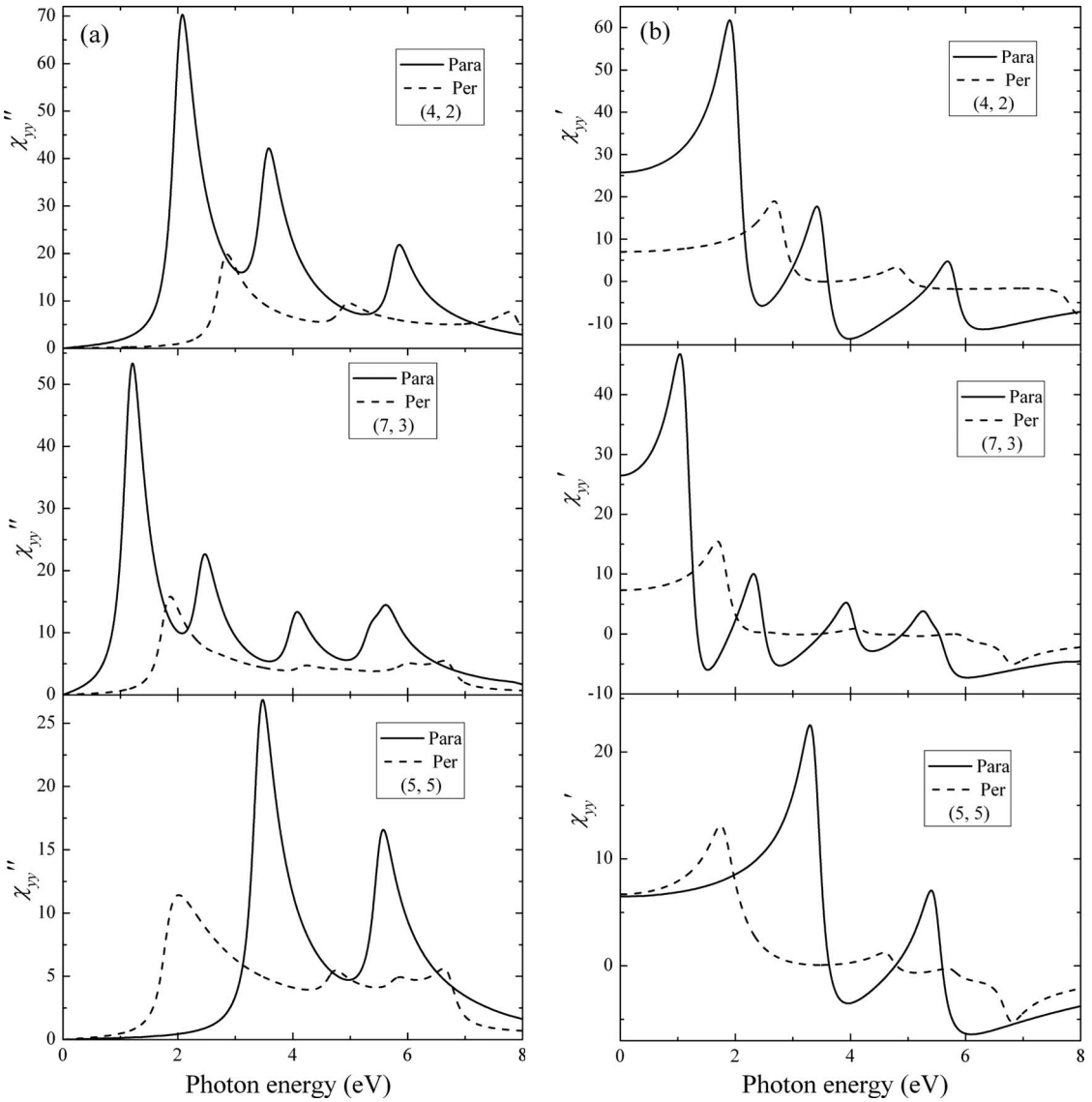

FIG. 4. (a) The imaginary (χ''_{yy}) and (b) real (χ'_{yy}) parts of the susceptibility of some SWCNs for parallel (Para) and perpendicular (Per) polarization.

tum matrix element for chiral CNs, e.g., (4, 2) CN in Fig. 3. The plot shows the full symmetrical behavior of the system in the first Brillouin zone and moreover enables us to study the momentum vector including all transition bands even in complicated chiral CNs. Using Eq. (24), one is able to reduce huge amount of numerical calculations and obtain the optical properties of CNs semianalytically. In the following, we use Eq. (24) to obtain the short axis linear susceptibility for arbitrary (n,m) SWCNs.

V. SHORT AXIS LINEAR SUSCEPTIBILITY

Using the diagonal components of the linear susceptibility given by[12]

$$\chi_{ii}(\omega) = \frac{2}{\pi\varepsilon_0 A}\sum_{c,v}\int_{-\pi/T}^{\pi/T}|d^i_{c,v}(\vec{k})|^2\frac{E_{cv}(k)dk}{E^2_{cv}(k)-\hbar^2\Omega^2}, \quad (25)$$

the y component of the short axis linear susceptibility is given by

$$\chi_{yy}(\omega) = \frac{e^2\gamma_0^2}{\pi\varepsilon_0 A}\delta_{K_2K'_2}\sum_{\mu,\mu'=0}^{N-1}\delta_{\mu'=\mu\pm1}\int_0^{\pi/T}|v^{A_0}_{\pm}|^2 \times\sin\left[\frac{2\varphi_{\pm}(\vec{k})-\varphi_c(\vec{k}')-\varphi_v(\vec{k})}{2}\right]^2 \times\frac{dK_2}{E_{cv}(k)(E^2_{cv}(k)-\hbar^2\Omega^2)}. \quad (26)$$

Due to the complicated $\vec{k}$ dependence of the sin term as well as the transition energies, no analytic solution has been found for this integral. In the form given above, however, the integral is easily computed numerically. The importance of knowing the absorption spectra from isolated SWCNs for both parallel and perpendicular polarization has been pointed out in a resonance Raman studies of SWCNs.[29] They showed that resonance Raman scattering from cross polarized light involving the $E_{\mu,\mu\pm1}$ van Hove singularities in the joint den-

sity of states also needs to be taken into account when analyzing Raman spectra from isolated SWCNs.

To show the polarization-dependent optical properties of CNs we plot χ_{yy} for both real and imaginary parts of some CNs (4, 2), (7, 3), and (5, 5) in Fig. 4. The peaks for parallel polarization originate from minima and maxima of occupied and unoccupied bands with the same energy subband indices. However, those for perpendicular polarization originate from minima and maxima of occupied and unoccupied bands with different energy subband indices. It is seen that the resonance energy positions are different for different polarization directions and moreover in the perpendicular case the susceptibility is made up of a broad hump in agreement with our previous work.[28] It should be mentioned that we do not consider the depolarization effect.[30–33] It is also noted that for both cases the intraband transitions have not been taken into account. Hence, for metallic CNs in the case of perpendicular polarizations a resonance peak appears at lower energy than that of the parallel polarization. This peak is created by the transitions originating from valence band lower than the band crosses the Fermi level to the conduction band which passes through the Fermi level. If intraband transitions are taken into account there will be a high-resonance peak at very low energy for the case of parallel polarization.

VI. CONCLUSION

Using the tight-binding approximation we have calculated the optical matrix elements of single wall carbon nanotubes with arbitrary chirality for linearly polarized light with polarization perpendicular to the nanotube axis. The significant k dependence of dipole matrix elements means their inclusion cannot be ignored in accurate calculations of the optical response. Moreover, we have studied the short axis linear susceptibility semianalytically.

*zarifi@mail.yu.ac.ir

[1] M. Ichida, S. Mizuno, Y. Saito, H. Kataura, Y. Achiba, and A. Nakamura, Phys. Rev. B **65**, 241407 (2002).
[2] Z. M. Li, Z. K. Tang, H. J. Liu, N. Wang, C. T. Chan, R. Saito, S. Okada, G. D. Li, J. S. Chen, N. Nagasawa, and S. Tsuda, Phys. Rev. Lett. **87**, 127401 (2001).
[3] S. M. Bachilo, M. S. Strano, C. Kittrell, R. H. Hauge, R. E. Smalley, and R. B. Wiesman, Science **298**, 2361 (2002).
[4] J. Jiang, J. Dong, and D. Y. Xing, Phys. Rev. B **59**, 9838 (1999).
[5] M. F. Lin and Kenneth W.-K. Shung, Phys. Rev. B **50**, 17744 (1994).
[6] M. F. Lin, F. L. Shyu, and R. B. Chen, Phys. Rev. B **61**, 14114 (2000).
[7] S. Tasaki, K. Maekawa, and T. Yamabe, Phys. Rev. B **57**, 9301 (1998).
[8] VI. A. Margulis and E. A. Gaiduk, Chem. Phys. Lett. **341**, 16 (2001).
[9] G. Ya. Slepyan, S. A. Maksimenko, A. Lakhtakia, O. Yevtushenko, and A. V. Gusakov, Phys. Rev. B **60**, 17136 (1999).
[10] G. Y. Guo, K. C. Chu, D. S. Wang, and C. G. Duan, Phys. Rev. B **69**, 205416 (2004).
[11] R. Saito, A. Grüneis, G. G. Samsonidze, G. Dresselhaus, M. S. Dresselhaus, A. Jorio, L. G. Cancado, M. A. Pimenta, and A. G. Souza Filho, Appl. Phys. A: Mater. Sci. Process. **78**, 1099 (2004).
[12] A. Zarifi and T. G. Pedersen, Phys. Rev. B **74**, 155434 (2006).
[13] S. V. Goupalov, Phys. Rev. B **72**, 195403 (2005).
[14] J. Jiang, R. Saito, A. Grüneis, G. Dresselhaus, and M. S. Dresselhaus, Carbon **42**, 3169 (2004).
[15] E. Malić, M. Hirtschulz, F. Milde, A. Knorr, and S. Reich, Phys. Rev. B **74**, 195431 (2006).
[16] Y. Hashimoto, Y. Murakami, S. Maruyama, and J. Kono, Phys. Rev. B **75**, 245408 (2007).
[17] Y. Murakami, E. Einarsson, T. Edamura, and S. Maruyama, Carbon **43**, 2664 (2005).
[18] A. Grüneis, R. Saito, Ge. G. Samsonidze, T. Kimura, M. A. Pimenta, A. Jorio, A. G. Souza Filho, G. Dresselhaus, and M. S. Dresselhaus, Phys. Rev. B **67**, 165402 (2003).
[19] M. F. Islam, D. E. Milkie, C. L. Kane, A. G. Yodh, and J. M. Kikkawa, Phys. Rev. Lett. **93**, 037404 (2004).
[20] G. S. Duesberg, I. Loa, M. Burghard, K. Syassen, and S. Roth, Phys. Rev. Lett. **85**, 5436 (2000).
[21] J. Hwang, H. H. Gommans, A. Ugawa, H. Tashiro, R. Haggenmueller, K. I. Winey, J. E. Fischer, D. B. Tanner, and A. G. Rinzler, Phys. Rev. B **62**, R13310 (2000).
[22] M. Ichida, S. Misuno, H. Kataura, Y. Achiba, and A. Nakamura, Appl. Phys. A: Mater. Sci. Process. **78**, 1117 (2004).
[23] V. N. Popov and L. Henrard, Phys. Rev. B **70**, 115407 (2004).
[24] J. W. Mintmire and C. T. White, Phys. Rev. Lett. **81**, 2506 (1998).
[25] R. Saito, G. Dresselhaus, and M. S. Dresselhaus, Phys. Rev. B **61**, 2981 (2000).
[26] S. Reich, J. Maultzsch, C. Thomsen, and P. Ordejón, Phys. Rev. B **66**, 035412 (2002).
[27] R. Saito, G. Dresselhaus, and M. S. Dresselhaus, *Physical Properties of Carbon Nanotubes* (Imperial College Press, U.K., 2003).
[28] A. Zarifi and T. G. Pedersen, J. Phys.: Condens. Matter **20**, 275211 (2008).
[29] A. Jorio, M. A. Pimenta, A. G. Souza Filho, Ge. G. Samsonidze, A. K. Swan, M. S. Ünlü, B. B. Goldberg, R. Saito, G. Dresselhaus, and M. S. Dresselhaus, Phys. Rev. Lett. **90**, 107403 (2003).
[30] A. Jorio, G. Dresselhaus, M. S. Dresselhaus, M. Souza, M. S. S. Dantas, M. A. Pimenta, A. M. Rao, R. Saito, C. Liu, and H. M. Cheng, Phys. Rev. Lett. **85**, 2617 (2000).
[31] A. M. Rao, A. Jorio, M. A. Pimenta, M. S. S. Dantas, R. Saito, G. Dresselhaus, and M. S. Dresselhaus, Phys. Rev. Lett. **84**, 1820 (2000).
[32] Z. Yu and L. Brus, J. Phys. Chem. B **105**, 1123 (2001).
[33] A. Jorio, A. G. Souza Filho, V. W. Brar, A. K. Swan, M. S. Ünlü, B. B. Goldberg, A. Righi, J. H. Hafner, C. M. Lieber, R. Saito, G. Dresselhaus, and M. S. Dresselhaus, Phys. Rev. B **65**, 121402(R) (2002).